CHEMICAL & PHARMACEUTICAL BULLETIN

Vol. 30, No. 5 May 1982

Regular Articles

[Chem. Pharm. Bull. 30(5)1539—1549(1982)]

Oxidation of Glucose on Immobilized Glucose Oxidase in a Trickle-Bed Reactor: Effect of Liquid-Solid Contacting Efficiency on the Global Rate of Reaction[1)]

Toyohisa Tsukamoto, Shushi Morita, and Jutaro Okada*

Faculty of Pharmaceutical Sciences, Kyoto University, Yoshida-Shimoadachi-cho, Sakyo-ku, Kyoto, 606, Japan

(Received October 16, 1981)

Oxidation of glucose to gluconic acid using a catalyst consisting of glucose oxidase and catalase both immobilized on activated carbon was employed to study the liquid-solid contacting efficiency (f) in a trickle-bed reactor. The global rates of reaction were measured at 25°C and at atmospheric pressure, as a function of catalyst loading (1.0 to 9.0 g), catalyst particle size (0.055 and 0.110 cm), superficial liquid velocity (0.044 to 0.337 cm/s), and superficial gas velocity (1.63 to 7.35 cm/s). The measured rate was considered to be the sum of the rates at the liquid-covered and gas-covered outer surfaces of catalyst particles. The value of f was determined by integrating numerically the mass balance equations for oxygen and the equation for the intrinsic rate of reaction simultaneously. The estimated value of f did not vary with catalyst loading. While f was independent of gas flow rates, it was influenced by both liquid flow rates and particle sizes. The effects of these operating parameters on f are discussed on the basis of the static and/or dynamic holdup.

Keywords——trickle-bed reactor; contacting efficiency; oxidation; glucose; immobilized enzyme catalyst; glucose oxidase; catalase; activated carbon; mass transfer; liquid-full reactor

It is well known that the liquid-solid contacting efficiency (the fraction of the particle surface covered by liquid) is one of the most important factors which influence the global rates of reaction in trickle-bed reactors where liquid and gas phases flow concurrently downward over a bed of catalyst particles. While there are many reports about the liquid-solid contacting efficiency, these are fragmentary, especially with respect to the effect of liquid flow rates. In previous work,[2)] experiments were performed without any mass transfer resistance, and the liquid-solid contacting efficiency was 0.91 and did not vary with liquid flow rates. One objective of this work was to compare the liquid-solid contacting efficiency under conditions of mass transfer resistances with that obtained in the previous work.[2)] Another objective was to develop design equations for trickle-bed reactors.

The oxidation of glucose to gluconic acid using a catalyst consisting of glucose oxidase and catalase both immobilized on activated carbon was chosen. Our work was done with a relatively active immobilized enzyme catalyst, at 25°C and at atmospheric pressure. The intrinsic kinetics of this reaction measured in free enzyme solution and the intraparticle mass transfer of dissolved oxygen in the liquid were reported in the preceding paper.[3)] The global rates of reaction were determined from the absorption rates of oxygen gas. The liquid-solid

contacting efficiency determined from the rate data was independent of gas flow rates, but varied with both liquid flow rates and particle sizes.

Experimental

Preparation of Immobilized Enzyme Catalyst——The immobilized enzyme catalyst was prepared in the same manner as described in the preceding paper.[3] In this study, two average particle sizes of activated carbon were chosen for the support: $d_P=0.055$ cm (28 to 32 mesh) and $d_P=0.110$ cm (14 to 16 mesh). To achieve covalent enzyme linkage to the support, the carbodiimide method was employed.[4] For one gram of activated carbon (dry weight basis), 70 mg of glucose oxidase (from *Aspergillus niger*, Sigma Chemical Company, 25,600 units/g stated activity), and 20 mg of catalase (from bovine liver, Sigma Chemical Company, 2,000 units/mg stated activity) were used. The physical properties of the immobilized enzyme catalyst were shown in Table I of the preceding paper.[3]

Apparatus and Operating Procedure——Fig. 1 shows a schematic diagram of the apparatus used. The glass reactor 1 was 2.1 cm i.d. and 27 cm long. In a constant temperature bath 4, 0.1 M glucose (in 0.1 M acetate buffer) solution contained in reservoir 3 was saturated with oxygen gas by continuous bubbling.

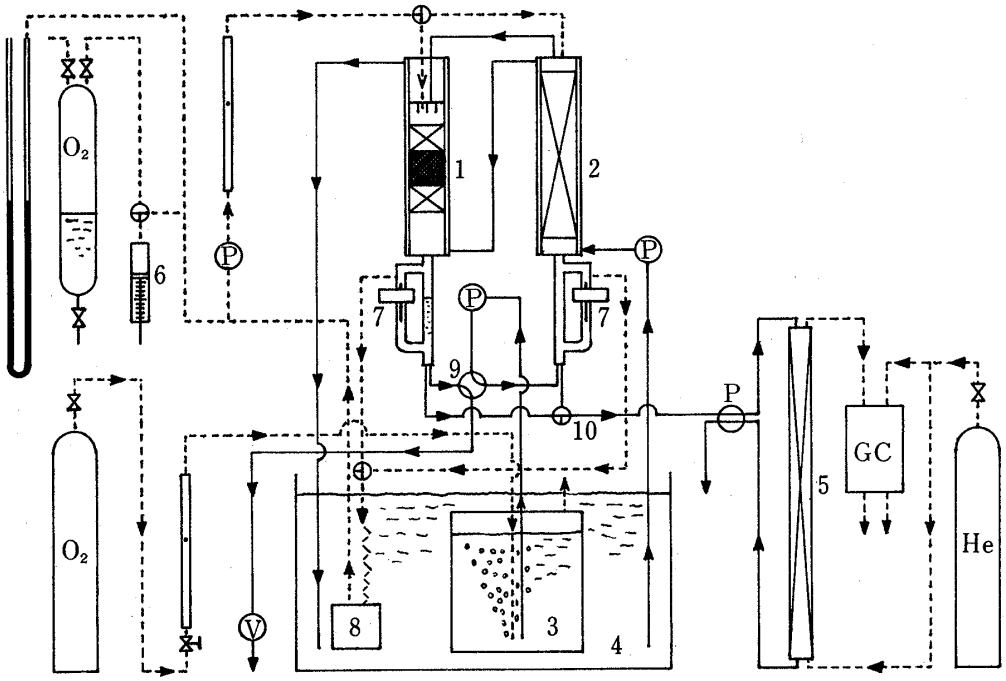

Fig. 1. Schematic Diagram of the Trickle-Bed Reactor used

——→——, gas flow line; ——→——, liquid flow line.
1, trickle-bed (or liquid-full) reactor; 2, heat exchanger (for trickle-bed operation) or absorber (for liquid-full operation); 3, glucose solution reservoir; 4, constant temperature bath; 5, stripping column; 6, piston burette; 7, level controller; 8, flask; 9, four-way valve; 10, three-way valve; P, pump; V, solenoid valve; GC, gas chromatograph.

For trickle-bed operation, the glucose solution and oxygen gas which was circulating in the reaction system were introduced into the top of the reactor, where the temperature was kept constant by circulating water from the constant temperature bath through the jacket. In the reactor, the glucose solution was introduced into the catalyst bed through a distributor consisting of three 0.1 cm i.d. and 1.0 cm long capillary tubes (stainless steel) placed across the reactor cross-section. The outlet of the tubes was located 0.5 cm above the top of the carbon prepacking. The bed as a whole consisted of three sections: a prepacking section of carbon particles, a catalyst section of immobilized enzyme on carbon particles, and an aftersection of carbon particles, all supported by a stainless steel screen placed 6 cm above the bottom of the reactor. The particle sizes, the lengths of these sections and other experimental conditions are presented in Table I. On the basis of the criteria reported by Herskowitz *et al.*[5] for uniform liquid distribution throughout the catalyst section, it was expected that with this arrangement the radial dispersion would be negligible.

After passing through the reactor, the effluent was separated into gas and liquid phases in the gas-liquid separator, which was located at the bottom of the reactor. In the separator, the liquid level was kept constant by the solenoid valve V, connected to a photo-electric switch. A part of the separated glucose solution was

Table I. Experimental Conditions

	Trickle-bed reactor	Liquid-full reactor
Diameter of catalyst particle, d_P, cm	0.055[a], 0.110[b]	0.110[b]
Length of pre- and after packing sections, cm	2.31	2.31
Length of catalyst section, cm	0.77, 2.31, 6.94	0.77
Mass of catalyst in reactor, m, g	1.0, 3.0, 9.0	1.0
Superficial liquid velocity, u_L, cm/s	0.044—0.337	0.042—0.131
Superficial gas velocity, u_G, cm/s	1.63—7.35	
Reaction temperature, °C	25	25

a) 28 to 32 mesh.
b) 14 to 16 mesh.

fed to the top of a stripping column 5 for gas chromatographic analysis of oxygen, and the rest was discharged through the solenoid valve.

In the stripping column, which was a 1.6 cm i.d. and 100 cm long column packed with 2—4 mm glass beads, helium was used to remove dissolved oxygen from the glucose solution. A 2 ml aliquot of the mixed gas from the stripping column was passed to a gas chromatograph GC with a 100 cm long and 0.4 cm o.d. stainless steel column packed with 5A molecular sieve particles (80—100 mesh). The column was maintained at 50°C. Then, the concentration of oxygen was measured by comparing the peak area for the effluent stream from the reactor with that for distilled water saturated with oxygen at the reaction temperature. The concentration of oxygen in the feed stream to the reactor was also measured in the same manner, by turning the three-way valve 10.

The gas separated in the gas-liquid separator was circulated by the pump through a flask 8 immersed in the constant temperature bath. The volume of oxygen absorbed by the reaction was measured by means of a piston burette 6. As can be seen from Fig. 1, the circulating gas was kept at atmospheric pressure by supplying oxygen from the burette.

For liquid-full operation, the same glucose solution was fed from the bottom of the reactor 1, by turning the four-way valve 9 through 90°. The effluent was then introduced into the top of the absorber 2, which was a 1.5 cm i.d. and 25 cm long glass column packed with 2—3 mm glass beads. The temperature of the absorber was also kept constant by circulating water from the constant temperature bath through the jacket. In the absorber the glucose solution was concurrently brought into contact with the circulating oxygen gas, so that most of the oxygen consumed in the liquid-full reactor was supplied from the flowing oxygen gas to the glucose solution. At the bottom of the absorber, the gas-liquid separator with the level controller 7 was placed. Other details were the same as for trickle-bed operation.

Results and Discussion

Global Rate of Reaction

Considering the operating procedure described in the experimental section, the global rate of reaction in the reactor, R [mol/s], can be calculated from the amount of oxygen absorbed during a certain period, t [s], and the difference between the dissolved oxygen concentrations in the feed stream to the reactor, C_f [mol/cm^3], and in the effluent stream from the gas-liquid separator, C_e [mol/cm^3]. Then, R may be written as

$$R = \frac{M_{O_2}}{t} + (C_f - C_e) \cdot Q_L \qquad (1)$$

where Q_L [cm^3/s] is the volumetric feed rate of glucose solution. M_{O_2} [mol], which is the number of moles of oxygen gas supplied by the piston burette during a run, can be evaluated from the gas law with the correction based on the vapor pressure of water at room temperature.

First, the activity of the immobilized enzyme catalyst was followed by measuring the global rates of reaction under the fixed experimental conditions for a period of 12 h. The activity was almost constant during measurements. Since, during the period, more than 30 l of glucose solution was passed through a bed consisting of only 1 g of catalyst particles, it was considered that the enzymes were surely bound covalently to activated carbon. If they were

physically adsorbed in the pores of activated carbon, the activity should decrease with time.

In the present study, for both trickle-bed and liquid-full operations, the conversion of glucose after passage through the reactor was adjusted to be small enough to regard the glucose concentration as uniform throughout the reactor. Hence, both operations were regarded as differential with respect to glucose. However, owing to the high catalyst activity of immobilized enzymes, the slow mass transfer rate of oxygen from the gas to liquid phase and the low concentration of oxygen in the liquid (compared to the concentration of glucose), the changes in oxygen concentration along the axial position in the reactor were expected to be substantial, so that both operations were regarded as integral with respect to oxygen.

Mass Balance Equation for Oxygen inside the Catalyst Particles

Using the same immobilized enzyme catalyst as used in this work, the initial rates of reaction were measured in a stirred tank reactor, and the results were presented in the preceding paper.[3] The intrinsic rate of reaction on the immobilized enzyme catalyst was well experssed by the Michaelis Menten kinetics, and both the maximum velocity and the Michaelis constant were proportional to the concentration of oxygen in the liquid. Then, the mass balance equation inside the pores in the catalyst particles can be written as

$$\frac{\partial^2 C_i}{\partial r^2} + \frac{2}{r}\cdot\frac{\partial C_i}{\partial r} - \frac{\rho_P}{D_e}\cdot\frac{kC_i\cdot(C_A)_L}{(KC_i+(C_A)_L)} = 0 \qquad (2)$$

where C_i [mol/cm^3] is the concentration of oxygen inside the pores in the catalyst particle, r [cm] is the radial distance in the particle, ρ_P [g/cm^3] is the particle density, D_e [cm^2/s] is the effective diffusivity of oxygen in the liquid inside the pores, and k and K are the proportional coefficients of maximum velocity and Michaelis constant, respectively. As mentioned above, the glucose concentration in the liquid, $(C_A)_L$ [mol/cm^3], can be considered uniform throughout the trickle-bed reactor under our experimental conditions.

Mass Balance Equation for Oxygen in the Bulk Liquid

In Fig. 2, the global rates of reaction in the trickle-bed reactor, R_{TB} [mol/s], are plotted as a function of the superficial liquid velocity, u_L [cm/s], or the superficial gas velocity, u_G [cm/s]. For each catalyst loading, the global rates increase with increasing u_L and/or u_G. This indicates that the external mass transfers of oxygen are important. At a fixed velocity

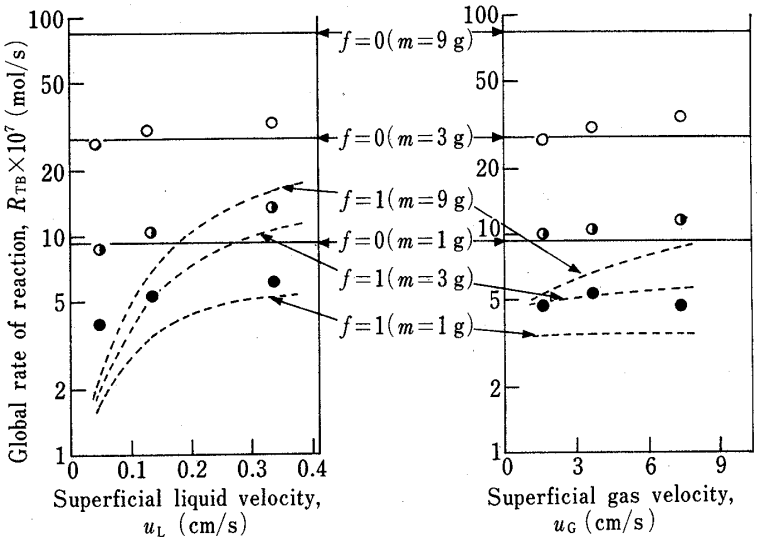

Fig. 2. Global Rate of Reaction in a Trickle-Bed Reactor *vs.* Superficial Liquid Velocity and Superficial Gas Velocity

d_P=0.055 cm; ○, m=9 g; ◑, m=3 g; ●, m=1 g.

of liquid or gas, the proportionality between R_{TB} and the catalyst loading, m [g], does not seem to be consistent, suggesting that the operation is integral.

The outer surface of the catalyst particles in trickle-bed reactors is not covered completely with the flowing liquid. The fraction, f [—], of the particle surface covered with liquid is defined as the liquid-solid contacting efficiency. As glucose is not a volatile reactant, gas phase reaction will not occur. Then, R_{TB} may be written as

$$R_{TB} = f \cdot R_{wet} + (1-f) \cdot R_{dry} \tag{3}$$

where R_{wet} [mol/s] and R_{dry} [mol/s] are the global rates of reaction on the catalyst covered and not covered with the flowing liquid, respectively. In this paper, the covered and not covered surfaces with the flowing liquid will be conveniently called the wet and dry surfaces, respectively. Under the fixed operating conditions, the value of f is regarded as uniform throughout the catalyst bed.[5]

According to Turek *et al.*[6] and Goto *et al.*,[7] the effect of axial dispersion on the concentration profile in the bulk liquid is expected to be negligible under our experimental conditions of liquid and gas flow rates. Thus, the liquid flow is considered to be plug flow. Therefore, for the wet surface of catalyst particles, in the steady state, the oxygen concentration in the bulk liquid, C_L [mol/cm^3], should be given by the following mass balance equation;

$$Q_L \frac{\partial C_L}{\partial z} + (k_L a_L) S (C_L^* - C_L) - (k_S a_S) S (C_L - C_S) = 0 \tag{4}$$

where z [cm] is the axial distance from the top of the catalyst bed, S [cm^2] is the cross-sectional area of the reactor, and C_L^* [mol/cm^3] and C_S [mol/cm^3] are the saturated concentration of oxygen in the liquid and the concentration of oxygen in the liquid at the surface of the particle, respectively. $(k_L a_L)$ [1/s] and $(k_S a_S)$ [1/s] are the gas-liquid and liquid-solid volumetric mass transfer coefficients, respectively.

As the feed solution to the reactor is saturated with oxygen,

$$C_L = C_L^* \qquad \text{at } z = 0 \tag{5}$$

At the center of the particle, the gradient of oxygen concentration will be zero because of the symmetry, so that

$$\frac{\partial C_i}{\partial r} = 0 \qquad \text{at } r = 0 \tag{6}$$

From the continuity of flux at the surface of the particle,

$$D_e \frac{\partial C_i}{\partial r} = k_S \cdot (C_L - C_S) \qquad \text{at } r = r_S \tag{7}$$

where k_S [cm/s] is the liquid-solid mass transfer coefficient.

Numerical Integration

The partial differential equations (2) and (4) with the boundary conditions (5) to (7) are difficult to solve analytically. Thus, these equations were integrated numerically to estimate the global rate of reaction at wet surface, R_{wet}. The values of k, K and D_e in equation (2) were obtained in the preceding work[3] (k=7.44 [cm^3/g-cat·s], K=84.8 [—] and D_e=7.80×10^{-6} [cm^2/s]). The values of $k_L a_L$ and $k_S a_S$ in equation (4) are also necessary for this integration.

Many correlations for $k_L a_L$ in trickle-bed reactors have been reported,[7-9] which were mainly based on studies of the desorption of gases from water. Most of them indicate that $k_L a_L$ is independent of the superficial gas velocity. For example, the following dimensional correlation was presented by Goto *et al.*[7];

$$k_L a_L = \alpha_L \cdot D \left(\frac{Q_L}{S \cdot \mu_L}\right)^{n_L} \left(\frac{\mu_L}{\rho_L \cdot D}\right)^{1/2} \tag{8}$$

where D [cm^2/s] is the molecular diffusivity in liquid, and the constants α_L [cm$^{n_L-2}$] and n_L [—] are related to the mass transfer surface and geometry of the particle and are specific for each packing. On the other hand, Sato *et al.*[8] presented the following dimensional correlation, where k_La_L depended on both superficial gas and liquid velocities:

$$k_La_L = 31 \cdot d_P^{-0.5} \cdot u_L^{0.8} \cdot u_G^{0.8} \tag{9}$$

where k_La_L is in [1/s], d_P is in [mm] and u_L and u_G are in [m/s].

There are also many available correlations for k_Sa_S in trickle-bed reactors.[7,10,11] These correlations were usually obtained from studies of the dissolution of organic particles (for example, benzoic acid or β-naphthol) in water. We used two correlations of Van Krevelen *et al.*[10] (eq. (10)) and Goto *et al.*[7] (eq. (11));

$$k_Sa_S = 1.8 \cdot D \cdot a_t^2 \left(\frac{u_L \cdot \rho_L}{\mu_L \cdot a_t}\right)^{1/2} \left(\frac{\mu_L}{\rho_L \cdot D}\right)^{1/3} \tag{10}$$

$$k_Sa_S = \alpha_S \cdot D \left(\frac{u_L \cdot \rho_L}{\mu_L}\right)^{n_S} \left(\frac{\mu_L}{\rho_L \cdot D}\right)^{1/3} \tag{11}$$

where a_t [1/cm] is the geometrical surface area of the particles per unit bed volume, and the constants α_S [cm$^{n_S-2}$] and n_S [—] have values specific for each packing. Supposing the particles are spherical, a_t can be written as

$$a_t = 6(1-\varepsilon_B)/d_P \tag{12}$$

where ε_B [—] is the void fraction of the bed. The effective liquid-solid interfacial area per unit bed volume, a_S [1/cm], can be calculated as the product of f and a_t:

$$a_S = f \cdot a_t \tag{13}$$

Substituting equation (12) into equation (13), and dividing k_Sa_S by the resultant a_S gives k_S as

$$k_S = \frac{k_Sa_S}{a_S} = \frac{(k_Sa_S) \cdot d_P}{6 \cdot f \cdot (1-\varepsilon_B)} \tag{14}$$

The procedure of numerical integration was as follows:

1. An arbitrary value of f was chosen.
2. For $z=z_1$ [$C_L=(C_L)_1$ at $z=z_1$, or $(C_L)_1=C_L{}^*$ at $z_1=0$ (boundary condition (5))], an arbitrary value of C_i at the center of the particle was chosen. Using the Runge–Kutta–Gill method, equation (2) was integrated with the known values of ρ_P, D_e, k, K and $(C_A)_L$. Since equation (2) does not hold at $r=0$, the calculation was started from $r=10^{-10} \cdot r_S$, where $\Delta C_i/\Delta r=0$ (boundary condition (6)). The increment Δr was chosen as $0.02 \cdot r_S$. By this calculation, the values of C_i and $\Delta C_i/\Delta r$ at $r=r_S$ were obtained. The integration was repeated until the boundary condition (7) was satisfied by changing the value of C_i at $r=10^{-10} \cdot r_S$; the value of k_S had been calculated from equation (14). In this step, the value of $(C_S)_1$ could be determined.
3. The increment of the catalyst bed length, Δz, was chosen as $0.05 \cdot z_B$, where z_B [cm] was the length of the bed. Giving the values of k_La_L, k_Sa_S, S, Q_L, Δz and $(C_L)_1$ and the value of $(C_S)_1$ obtained by step 2 into equation (4), $(\Delta C_L)_1$ was calculated. Then, the value of $(C_L)_2$ ($=(C_L)_1+(\Delta C_L)_1$) at the next bed length z_2 ($=z_1+\Delta z$) was calculated.
4. Steps 2 and 3 were repeated till $z_1=z_B$.

The differences in oxygen concentration in the liquid at the end of the catalyst bed (C_L at $z=z_B$) calculated by using $\Delta z=0.01 \cdot z_B$ and $\Delta r=0.01 \cdot r_S$, and using $\Delta z=0.05 \cdot z_B$ and $\Delta r=0.02 \cdot r_S$, was less than 1%, so that the errors inherent in calculation by the above procedure are negligible.

The global rate of reaction at the wet surface in the reactor R_{wet} [mol/s] can be expressed by

$$f \cdot R_{wet} = \frac{S \cdot f \cdot a_t \cdot D_e}{r_S} \int_0^{z_B} C_S \left(\frac{\partial C_i}{\partial r}\right)_{r=r_S} \cdot dz \qquad (15)$$

Using the Simpson rule the integral was evaluated numerically from the values of C_S and $\Delta C_i/\Delta r$ at r_S for each bed length, z, which had been obtained by step 2.

Contribution of the Dry Surface to the Global Rate of Reaction

In the previous work,[2] for the oxidation of glucose over Pt on activated carbon in a trickle-bed reactor, it was assumed that no reaction occurred at the dry surface of the catalyst particles, so that from eq. (3)

$$R_{TB} = f \cdot R_{wet} \qquad (3')$$

As there was no external mass transfer resistance with less active catalyst, R_{wet} was considered to be equal to the global rate of reaction in a liquid-full reactor, R_{LF} [mol/s]. Then,

$$R_{TB} = f \cdot R_{LF} \qquad (3'')$$

The data indicated that the average value of f obtained from equation (3″) was 0.91, independent of gas and liquid flow rates.

TABLE II. Calculated Values of the Global Rate of Reaction in a Trickle-Bed Reactor (for Run 322[a])[b]

Equation No. for k_La_L	(8)	(8)	(9)	(9)
Equation No. for k_Sa_S	(10)	(11)	(10)	(11)
$(R_{TB})_{calcd}$[c], mol/s	5.86×10^{-7}	5.46×10^{-7}	5.96×10^{-7}	5.53×10^{-7}
$(R_{TB})_{obsd}$[d], mol/s		1.91×10^{-6}		

a) Experimental conditions: diameter of catalyst particle, $d_P=0.110$ [cm]; amount of catalyst, $m=9.0$ [g]; superficial liquid velocity, $u_L=0.136$ [cm/s]; superficial gas velocity, $u_G=3.68$ [cm/s].
b) The value of f was assumed to be 0.91.
c) Calculated.
d) Observed.

First, to check the previous result, the global rates of reaction in the trickle-bed reactor were calculated under the assumptions of no reaction at the dry surface and $f=0.91$. Under our experimental conditions, eq. (9) gives 0.56—2.6 times larger values of k_La_L than eq. (8), and eq. (10) gives 1.5—4.3 times larger values of k_Sa_S than eq. (11). For a typical run, the evaluated values of R_{TB} using these mass transfer correlations are summarized in Table II (for run 322). The values of R_{TB} observed are more than three times higher than those calculated by using some combinations of correlations for k_La_L and k_Sa_S. For any run, even when the higher estimates for k_La_L and k_Sa_S are used, the calculated R_{TB} is at most 70% of the observed R_{TB}. Note that a higher volumetric coefficient gives a higher R_{TB}. Even at $f=1.0$, the calculated R_{TB} by using eqs. (9) and (10) is considerably less than the observed R_{TB}, as shown by the dotted lines in Fig. 2. The discre-

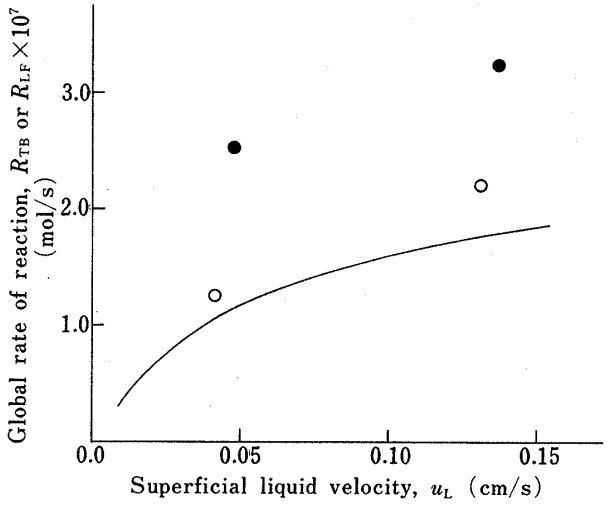

Fig. 3. Comparison of Global Rates of Reaction in Trickle-Bed and Liquid-Full Reactors

$d_P=0.110$ cm, $m=1$ g.
●, R_{TB}; ○, R_{LF}; ——, calculated curve.

pancy is too large to be explained by the uncertainties in k_La_L, k_Sa_S or other physical properties. The main reason for the difference between the observed and calculated values of R_{TB} is considered to be due to the assumption that no reaction occurs at the dry surface. Since the observed R_{TB} is considerably higher than the calculated R_{TB} even at f=1.0, the rate of reaction at the dry surface may make a relatively large contribution to the global rate of reaction. This can be indirectly confirmed by comparing the global rate of reaction in a trickle-bed reactor with that in a liquid-full reactor, both operated by using the same catalyst and under the same operating conditions except for the gas flow rate.

Liquid-Full Reactor Operation

The liquid-full runs were performed in the manner described in the experimental section. The results are shown in Fig. 3, together with the results of the trickle-bed runs. The trickle-bed reactor gives a higher global rate of reaction than the liquid-full reactor.

In the case of liquid-full operations, eq. (4) can be written as

$$Q_L \frac{\partial C_L}{\partial z} - (k_Sa_S)S(C_L - C_S) = 0 \qquad (4')$$

For the liquid-solid volumetric mass transfer coefficient in liquid-full reactors, the following correlation was presented by Dwivedi *et al.*[12] It is a reanalyzed one based on a number of previous experimental data.

$$k_Sa_S = \left\{\frac{0.765}{(Re_P)^{0.82}} + \frac{0.365}{(Re_P)^{0.365}}\right\}\frac{a_t}{\varepsilon_B} \cdot u_L(Sc)^{-2/3} \qquad (16)$$

where Re_P [—] is the Reynolds number based on the particle diameter ($=d_Pu_L\rho_L/\mu_L$) and Sc [—] is the Schmidt number ($=\mu_L/\rho_LD$). Equation (16) was used to estimate the global rate of reaction in the liquid-full reactor. Using the boundary conditions (5) to (7), eqs. (2) and (4') were integrated numerically in a manner similar to that mentioned above. Note that f is unity for liquid-full reactors.

The calculated R_{LF} is almost in accordance with the observed R_{LF}, as shown in Fig. 3. Therefore, the difference between the observed values of R_{TB} and R_{LF} at the same superficial liquid velocity indicates that the dry surface of catalyst particles contributes considerably to the global rate of reaction in the trickle-bed reactor, and that the overall rate of reaction at the dry surface is much larger than that at the wet surface. To analyze the experimental data for the hydrogenation of α-methylstyrene in a trickle-bed reactor, Morita *et al.*[13] and Herskowitz *et al.*[14] assumed that, at the dry surface, the gas-liquid and liquid-solid mass transfer resistances for the gaseous component (hydrogen) were negligible. The above assumption is reasonable because there is no flowing liquid on the dry surface, and because the flowing gas is in directly contact with the liquid near the pore mouth at the dry surface. It is also reasonable to assume that the catalyst pores under this dry surface are filled with the liquid by capillarity, and that the liquid is exchangeable because of the interconnection of the pores in the catalyst particles.

Liquid-Solid Contacting Efficiency in Trickle-Bed Reactor

Based on the assumptions mentioned in the preceding section, the equation describing R_{dry} will be derived. Since there is no external mass transfer resistance at the dry surface, equilibrium exists between the oxygen concentrations in the gas and in the liquid at the pore mouth; that is,

$$C_S = C_L^* \qquad \text{at } r = r_S \qquad (7')$$

Then, the rate of reaction per unit dry surface area will be uniform throughout the catalyst bed. This means that R_{dry} is proportional to the length of the catalyst bed. Thus, R_{dry} can be expressed as

$$R_{dry} = \frac{S \cdot z_B \cdot a_t \cdot D_e \cdot C_L^*}{r_S} \left(\frac{\partial C_i}{\partial r}\right)_{r=r_S} \quad (17)$$

where $(\partial C_i/\partial r)_{r=r_S}$ can be obtained by integrating eq. (2) with boundary conditions (6) and (7').

The values of R_{dry} calculated from eq. (17), which correspond to the global rates of reaction with no external mass transfer resistance, are shown as the solid lines in Fig. 2. Since $C_S = C_L^*$ at $r = r_S$, R_{dry} is independent of both u_L and u_G. All experimental R_{TB} are between R_{dry} and R_{wet} at $f=1$, indicating that $0<f<1$. Assigning an arbitrary value to f, eqs. (2), (3), (4) and (17) were numerically solved till the calculated R_{TB} agreed with the experimental R_{TB}. By this calculation, the value of f was determined for each run. The results for typical runs are summarized in Table III. As f is uniform throughout the catalyst bed, the calculated values of f should be independent of the amount of catalyst loading at the same gas and liquid flow rates. This can be well confirmed by comparing the values of f for $m=1$, 3 and 9 [g]. Table III also indicates that the values of f calculated from several combinations of correlations for k_La_L and k_Sa_S are nearly equal; that is, f is not very sensitive to the uncertainties in the mass transfer coefficients under our experimental conditions.

TABLE III. Calculated Values of f using some Combinations of Correlations for k_La_L and k_Sa_S

Equation No. for k_La_L Equation No. for k_Sa_S	(8) (10)	(8) (11)	(9) (10)	(9) (11)
Run 112 ($m=1.0$ g)[a]	0.65	0.59	0.64	0.59
Run 212 ($m=3.0$ g)[a]	0.69	0.67	0.68	0.67
Run 312 ($m=9.0$ g)[a]	0.65	0.64	0.66	0.63
Mean	0.65	0.64	0.66	0.63

a) Other experimental conditions: diameter of catalyst particle, $d_P=0.110$ [cm]; superficial liquid velocity, $u_L=0.048$ [cm/s]; superficial gas velocity, $u_G=3.68$ [cm/s].

In Fig. 4, the average of the values of f for $m=1$, 3 and 9 [g] obtained by using the correlations (9) and (10) is plotted against the superficial gas or liquid velocity. As shown in Fig. 4(a), f is independent of u_G. According to Satterfield,[15] Dianetto *et al.*[16] and Hirose *et al.*,[11] our experimental conditions were in the gas continuous regime. Certainly, pulsing or bubbling flow was not observed during our runs. It was also observed that the flow pattern in the bed did not change with gas flow rates. These observations indicate that the liquid-solid contacting efficiency may be independent of gas flow rates, in agreement with the experimental results. However, for particle sizes of $d_P=0.055$ [cm] and 0.110 [cm], the average values of f were 0.75 and 0.66, respectively.

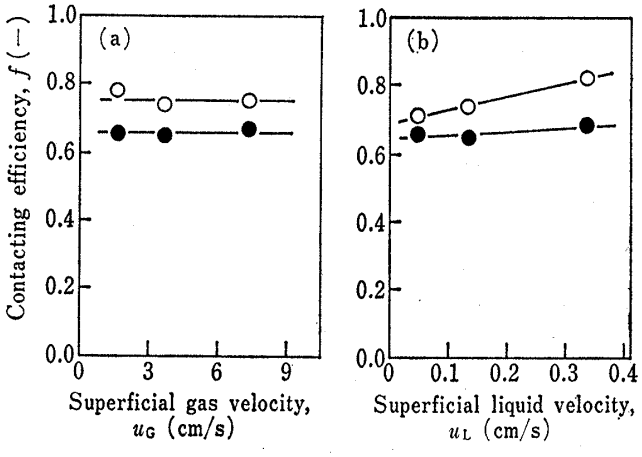

Fig. 4. Liquid-Solid Contacting Efficiency in a Trickle-Bed Reactor *vs.* Superficial Gas Velocity (a) and Superficial Liquid Velocity (b)
—○—, $d_P=0.055$ cm; —●—, $d_P=0.110$ cm.

The difference in f between particle sizes is most likely due to differences in static holdup, h_S [—]. Since the bulk densities of bed for both particle sizes were equal and the ratio of particle diameters was 1/2, the ratio of the numbers of particles per unit bed volume was 8/1. That is, the ratio of the numbers of contact points between particles was 8/1. Around each

contact point, a stagnant liquid zone exists, which contributes to h_S. This means that the outer surface around the contact point is covered with the liquid, or wet. The wetted area per one contact point for small particles may not differ too greatly from that for large particles, though the former may be less than the latter. Thus, the increase in the numbers of contact points will increase h_S, resulting in increase in the ratio of the wetted surface area to the total surface area of the catalyst particles, or f.

The dynamic holdup, h_D [—], is not affected by gas flow rates in trickle-bed reactors.[17] For this reason, the values of f would be independent of gas flow rates (Fig. 4(a)).

Next, the effect of liquid flow rates on f will be discussed. It is well known that h_D increases with liquid flow rate.[7,16,18] However, as shown in Fig. 4(b), in the case of large particles (d_P=0.110 cm) f is nearly constant. This can be explained by considering that increasing the liquid flow rate does not change the flow pattern in trickle-bed reactors but simply increases the liquid velocity and the thickness of the liquid rivulets. On the contrary, in the case of small particles, f increases with liquid flow rate. Owing to the limited inter-particle void space, the rivulets cannot increase in thickness with liquid flow rate, so that a part of the flowing liquid spreads over the dry surface. Thus, increasing the liquid flow rate increases f.

In the previous paper,[2] we reported that the liquid-solid contacting efficiency in a trickle-bed reactor was constant (f=0.91) regardless of liquid flow rates. This value was obtained by assuming that no reaction occurred at the dry surface. However, in the present experiments the observed R_{TB} was much larger than the observed R_{LF}. This result cannot be explained on the basis of that assumption. Since the previous experiments were performed without external mass transfer resistances, R_{wet} should be the same as R_{dry}, so that f=1. The result that f=0.91 can be considered to be consistent with unity, within the experimental errors.

Some of the available information about the liquid-solid contacting efficiency (f) is summarized in Fig. 6 of the previous paper.[2] Most of the values of f were between 0.6 and 1.0 in the range of u_L=0.05 to 0.5 [cm/s], and could be divided into two representative patterns. One is that f is independent of liquid flow rates, as presented by Schwartz *et al.*,[19] Morita *et al.*,[13] Hartman *et al.*,[20] *etc.* The other is that f increases with liquid flow rates, as presented by Satterfield,[15] Colombo *et al.*,[21] Herskowitz *et al.*,[14] *etc.* But, as far as as we know, no report has appeared on the effect of particle size on the contacting efficiency, especially in reaction systems. In this work, the effect of particle size on f is well explained by contact point and/or static holdup. Further, the effect of liquid flow rates on f can be explained as follows; for large particles, the increase in liquid flow rate does not change the flow pattern but simply increases the liquid velocity and the thickness of the liquid rivulets, so that f is independent of liquid flow rate. For small particles, increasing the liquid flow rate not only increases the liquid velocity and the thickness of the rivulets but also spreads out the flowing liquid over the dry surface, resulting in increase in f.

References and Notes

1) A part of this work was presented at the 101st Annual Meeting of the Pharmaceutical Society of Japan, Kumamoto-shi, Apr. 1981.
2) T. Tsukamoto, S. Morita, and J. Okada, *Chem. Pharm. Bull.*, **28**, 2188 (1980).
3) T. Tsukamoto, S. Morita, and J. Okada, *Chem. Pharm. Bull.*, **30**, 782 (1982).
4) Y.K. Cho and J.E. Bailey, *Biotechnol. Bioeng.*, **19**, 769 (1977).
5) M. Herskowitz and J.M. Smith, *A.I. Ch. E. Journal*, **24**, 439 (1978).
6) F. Turek and R. Lange, *Chem. Eng. Sci.*, **36**, 569 (1981).
7) S. Goto and J.M. Smith, *A.I. Ch. E. Journal*, **21**, 706 (1975).
8) Y. Sato, T. Hirose, F. Takahashi, and M. Toda: The 1st Pacific Chem. Eng. Congr., Paper 8–3 (1972).
9) N.D. Sylvester and P. Pitayagulsarn, *Ind. Eng. Chem. Process Des. Dev.*, **14**, 421 (1975); R.C. Ufford and J.J. Perona, *A.I. Ch. E. Journal*, **19**, 1223 (1973); K. Onda, E. Sada, and Y. Murase, *A.I. Ch. E. Journal*, **5**, 235 (1959); V.V. Mahajani and M.M. Sharma, *Chem. Eng. Sci.*, **34**, 1425 (1979).

10) D.W. Van Krevelen and J.T.C. Krekels, *Recl. Trav. Chim.*, **67**, 512 (1948).
11) T. Hirose, Y. Mori, and Y. Sato, *J. Chem. Eng. Japan*, **9**, 220 (1976).
12) P.N. Dwivedi and S.N. Upadhyay, *Ind. Eng. Chem. Process Des. Dev.*, **16**, 157 (1977).
13) S. Morita and J.M. Smith, *Ind. Eng. Chem. Fundamentals*, **17**, 113 (1978).
14) M. Herskowitz, R.G. Carbonell, and J.M. Smith, *A.I. Ch. E. Journal*, **25**, 272 (1979).
15) C.N. Satterfield, *A.I. Ch. E. Journal*, **21**, 209 (1975).
16) A. Gianetto, G.Baldi, V. Specchia, and S. Sicardi, *A.I. Ch. E. Journal*, **24**, 1087 (1978).
17) J.M. Hochman and E. Effron, *Ind. Eng. Chem. Fundamentals*, **8**, 63 (1969).
18) V. Specchia and G. Baldi, *Chem. Eng. Sci.*, **32**, 515 (1977).
19) J.G. Schwartz, E. Weger, and M.P. Duduković, *A.I. Ch. E. Journal*, **22**, 894 (1976).
20) M. Hartman and R.W. Coughlin, *Chem. Eng. Sci.*, **27**, 867 (1972).
21) A.J. Colombo, G. Baldi, and S. Sicardi, *Chem. Eng. Sci.*, **31**, 1101 (1976).